VOL 1, NO.1 (2021) 1-18
https://jagst.utm.my

JAGST
Journal of Advanced Geospatial Science & Technology

Assessment of Pine Forest Condition Towards Early Detection and Monitoring of Stress Through a Synergistic Use of Sentinel-1 and Sentinel-2 Imagery

Margaux Elijah P. Neri[1*], Bernadette Anne B. Recto[2], Ariel C. Blanco[1,2], and Roseanne V. Ramos[1,2]
[1]Department of Geodetic Engineering, University of the Philippines, Diliman, Quezon City, 1001, Philippines
[2]Training Center for Applied Geodesy and Photogrammetry, University of the Philippines, Diliman, Quezon City, 1001, Philippines.
*Corresponding author: mpneri1@alum.up.edu.ph

Abstract — An integrated use of Sentinel-1 Synthetic Aperture Radar (SAR) and Sentinel-2 multispectral imagery is implemented in this study for the assessment of pine forest condition in Camp John Hay, Baguio City, Philippines. These assessments include: (1) the inspection of distribution of dead trees, (2) trends analysis of Sentinel-derived products, and (3) the generation of anomaly maps. Dead trees were identified using Google Earth Pro imagery – the trees were classified as such if they manifest brown or grey foliage with evident foliage loss. The products used for succeeding analyses are sigma naught VH (σ^0_{VH}) and sigma naught VV (σ^0_{VV}) backscatter derived from Sentinel-1, Sentinel-2 bands 2, 3, 4, 5, 6, 7, 8, 8a, 11, and 12, as well as Sentinel-2 derived vegetation indices S2REP (Sentinel-2 Red-Edge Position Index), NDWI (Normalized Difference Water Index), NDVI (Normalized Difference Water Index), NDII (Normalized Difference Infrared Index), MSI (Moisture Stress Index), IRECI (Inverted Red-Edge Chlorophyll Index), GNDVI (Green Normalized Difference Water Index), and EVI (Enhanced Vegetation Index). Trends in these products were backtracked to identify patterns they exhibit as tree health deteriorates, and to determine which are most robust for early detection of stress in pine trees. From the analysis of slope decline against time, and their corresponding R^2 statistic, Sentinel-2 products found to be robust for early stress detection are band 5, followed by equally important GNDVI, NDII, MSI, and bands 2, 3, and 4, then NDVI. A synergistic analysis of Sentinel-1 and Sentinel-2 products showed that NDVI is well-correlated with σ^0_{VV} backscatter; hence, they exhibit concurrent decline in trends due to stress. Among Sentinel-1 products, a delayed decline in σ^0_{VH} backscatter occurred compared with σ^0_{VV} backscatter. These patterns manifested in three-month intervals. A map of high risk and low risk forest areas was generated from the overall average of negative and positive anomalies of vegetation indices. The relative reliability of the map of at-risk vegetation areas was computed based on the count of layer values with valid data per cell, resulting in a maximum relative reliability of 65.3%. This study showed that the integration of Sentinel-1 SAR and Sentinel-2 multispectral imagery is a promising approach in the comprehensive assessment of pine forest condition towards the early detection and monitoring of stress.

Keywords - Anomaly Map, SAR, Multispectral, Backscatter, Vegetation Indices

Article History: Received 22 December 2020, Accepted 30 May 2021, Published 1 August 2021

How to cite: Neri, M.E.P, Recto, B.A.B, Blanco, A.C., Ramos, R.V. (2021). Assessment of Pine Forest Condition Towards Early Detection and Monitoring of Stress Through a Synergistic Use of Sentinel-1 and Sentinel 2 Imagery. Journal of Advanced Geospatial Science & Technology 1(1), 1-18.

1.0 Introduction

Remote Sensing (RS) technology is used to acquire information about objects and phenomena on the surface of the Earth from a distance. One of the key applications of RS is in the field of forestry. Traditionally, forest covers were assessed by screening large areas to inspect trees; however, these methods are prone to be time-consuming, and generally show low efficiency (Abdullah et al., 2018 and Zhang et al., 2017). With RS, forest resource information over vast areas can be inventoried without laboriously taking direct measurements on the field (Arellano et al., 2019). RS also proves suitable for recording disturbance processes to forest health which is not sufficiently possible with terrestrial surveys (Lausch et al., 2016). Whereas in-situ forest inventories are insufficient to assess abrupt changes in forest health, RS technologies can monitor forest health indicators effectively, repetitively, and comparatively (Lausch et al., 2017).

The development of a monitoring system involving the synergy of in-situ terrestrial observations and RS technologies is crucial to forest health assessment and understanding the influence of stress inducers (Lausch et al., 2016). Light Detection and Ranging (LiDAR), Radio Detection and Ranging (RADAR), hyperspectral and integrated systems on Unmanned Aerial Vehicles (UAV), aircraft, space-borne, and close-range platforms are increasingly being established to support forest health observations (Lausch et al., 2017). Aerial images are among the most widely used RS data for forest health assessments (Hawrylo et al., 2018). RADAR data is known for its potential to map vegetation cover in regions with frequent cloud cover such as tropical and boreal forests, as well as its capability to provide time-series data with high calibration stability. In addition to being almost impervious to weather conditions, Synthetic Aperture RADAR (SAR) data provides information on the structure and moisture status. The complementary use of SAR and optical sensors helps improve mapping accuracy (Dostálová et al., 2016 and Bao et al., 2019). The Sentinel satellite constellation has both SAR and multispectral sensor systems with the key advantage of a full open access distribution of its products. Sentinel-1 satellites perform C-band SAR imaging which allows operation at wavelengths without cloud obstruction or lack of illumination. It offers reliable data acquisition and wide area monitoring under various weather conditions. On the other hand, the Sentinel-2 mission consists of two satellites namely, Sentinel-2A and Sentinel-2B, provides multispectral imagery containing red-edge spectral bands which extends the potential of Sentinel-2 products for vegetation analysis. The exploration of open-access satellite imagery such as Sentinel-1 and Sentinel-2 data provides great opportunities for comprehensive assessments of vegetation.

They offer high spatial and spectral resolutions with short revisit times which are deemed suitable for in-depth monitoring of large vegetation covers. Their spatial resolutions, however, pose limitations for assessment at the level of individual trees. Tree-level assessments using Sentinel products are not usually investigated; hence, extensive, and intensive exploration of their potential on the matter is well anticipated.

This study aims to integrate Sentinel-1 and Sentinel-2 imagery for the assessment of pine forest condition. Specifically, the objectives of this study are to: (1) backtrack the behaviour of SAR backscatter, bands, and vegetation indices (VIs) on individual trees to determine which products are suitable for early stress detection; and, (2) map at-risk forest areas using anomaly maps to provide priority recommendation for management and intervention. The study was motivated by the need for recommendations on managing forests under community quarantine restrictions brought about by the COVID-19 pandemic to be used by local agencies.

2.0 Materials and methods

2.1 Study area

The site used in the study is the Camp John Hay Special Economic Zone in Baguio City, Benguet Province, Philippines (Figure 1). It is a 213-hectare tourist destination and forest watershed reservation located in the regional centre of the Cordillera Administrative Region in the Philippines, between 16°23'49.3"N (longitude) and 120°36'40.9"E (latitude). The city's climate is characterised by a relatively low temperature all year round due to its geographic location. The average temperature ranges from 15 to 23 degrees Celsius, with the months of November to February bearing the lowest temperature recordings (Parao et al., 2019).

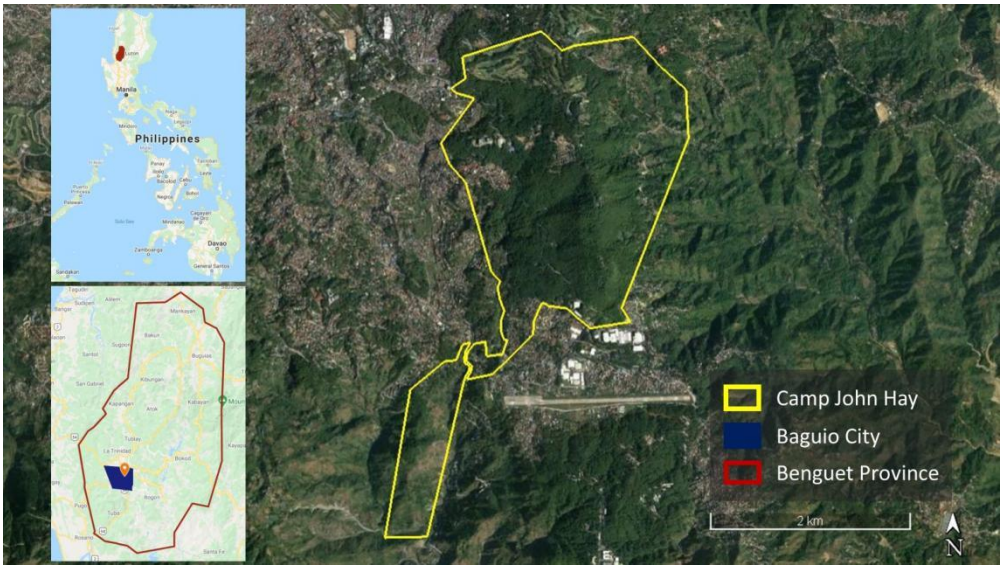

Figure 1. Location and boundaries of the study area, Camp John Hay Special Economic Zone, Baguio City. (source: Adapted from Google Earth and Google Maps Imagery - inset).

2.2 Satellite image processing

A total of seventeen (17) Sentinel-1 images were selected from 2016 to 2020 in 3-month intervals. The pre-processing workflow consists of orbit file application, thermal noise removal, radiometric calibration to convert digital number (DN) pixel values to radar backscatter, speckle filtering, terrain correction, and converting linear to sigma naught decibel (dB) values. The pre-processed images contain bands sigma naught VH (σ^0_{VH}) and sigma naught VV (σ^0_{VV}). Ten (10) Sentinel-2 images from 2017 to 2020 with 3-month intervals were used. The selected Sentinel-2 images were paired with available Sentinel-1 imagery with the closest sensing dates. Sentinel-2 pre-processing includes atmospheric correction using the Sen2Cor plugin from the Sentinel Application Platform (SNAP) software, and resampling of the bands to identical 10-meter resolutions. In total, ten (10) bands were derived as shown in Table 1. Sentinel-2 bands 1, 9, and 10 were excluded in this study since they are not used for vegetation mapping due to their sensitivity to aerosol.

VIs with the best capacity to detect and assess stress in vegetation were selected from published works to be used in this study (Table 2.). Parao et al. (2019), pointed out that most pine tree deaths in Camp John Hay are due to bark beetle infestation; hence, VIs with the ability to detect and map bark beetle occurrence were given more emphasis in this study.

Table 1. Sentinel-2 band characteristics.

Band	Description	Wavelength (nm)	Bandwidth (nm)
2	Blue	496.6	98
3	Green	560.0	45
4	Red	664,5	38
5	Vegetation Red Edge	703.9	19
6	Vegetation Red Edge	740.2	18
7	Vegetation Red Edge	782.5	28
8	NIR	835.1	145
8a	Narrow NIR	864.8	33
11	SWIR (2)	1613.7	143
12	SWIR (3)	2202.4	242

Table 2. Vegetation indices used for stress assessment.

VIs	Equation	Reference
Normalized Difference Vegetation Index (NDVI)	$\frac{\mathrm{NIR}-\mathrm{Red}}{\mathrm{NIR}+\mathrm{Red}}$	Bao et al. 2019; Braun, Fakhri, and Hochschild 2019
Green Normalized Difference Vegetation Index (GNDVI)	$\frac{\mathrm{NIR}-\mathrm{Green}}{\mathrm{NIR}+\mathrm{Green}}$	Frampton et al. 2013
Enhanced Vegetation Index (EVI)	$\frac{\mathrm{G}(\mathrm{NIR}-\mathrm{Green})}{\mathrm{NIR}+(\mathrm{C1})(\mathrm{Red})-(\mathrm{C2})(\mathrm{Blue})+\mathrm{l}}$	Bao et al. 2019; Frampton et al. 2013; Semeraro et al. 2020
Inverted Red Edge Chlorophyll Index (IRECI)	$\frac{\mathrm{NIR\text{-}Red}}{(\mathrm{RE}_1/\mathrm{RE}_{2)}}$	Frampton et al. 2013
Sentinel-2 Red Edge Chlorophyll Index (S2REP)	$705+35\left[\frac{\left(\frac{\mathrm{NIR}+\mathrm{Red}}{2}\right)-\mathrm{RE}_1}{\mathrm{RE}_1-\mathrm{RE}_2}\right]$	Frampton et al. 2013
Moisture Stress Index (MSI)	$\frac{\mathrm{SWIR}_1}{\mathrm{NIR}}$	Sanguesa-Barreda et al. 2014
Normalized Difference Infrared Index (NDII)	$\frac{\mathrm{NIR}-\mathrm{SWIR}_1}{\mathrm{NIR}-\mathrm{SWIR}_2}$	Sanguesa-Barreda et al. 2014
Normalized Difference Water Index (NDWI)	$\frac{\mathrm{Green}-\mathrm{NIR}}{\mathrm{Green}+\mathrm{NIR}}$	Semeraro et al. 2020

2.3 Geotagging of dead trees

Google Earth imagery was utilised to identify and geotag dead trees in the study area. The most recent historical image available with good enough resolution to spot dead trees in the study area was captured on February 20, 2018. Dead trees were classified as such if they appear with brown or grey foliage texture, or without leaves. Dead trees were geotagged by enclosing their overhead features with polygons.

2.4 Trends analysis

The polygons geotagged in Google Earth were converted to vector shapefile and imported in SNAP. The time-series feature was applied to visualise the trends of Sentinel products within the polygon vectors. Historical Google Earth imagery was explored to keep track of the health status of trees over time. The span of tree health deterioration varies per tree; hence, the timeline of interest for analysis differs from one tree to another. Trends in SAR backscatter, multispectral bands, and VIs were backtracked to identify patterns they exhibit during the deterioration phase of trees, to determine which manifests the earliest decline and which products are robust for early stress detection. Trees with timelines of interest not documented from early 2015 to early 2018 were automatically excluded for analysis.

Since backscatter values are heavily influenced by foliage volume and surface texture, it is expected that backscatter trends will decline as tree health deteriorates. To verify if backscatter decline occurred because of foliage loss, LAI trends were compared with that of backscatter. A simultaneous decline between LAI and backscatter is assumed to signify foliage loss. For the bands and VIs, the slopes of their overall decline were examined if the trees exhibit a consistent amount of decline in values as their health deteriorates. R^2 values of the overall decline over time were also computed to confirm the consistency displayed in the slope analysis. The R^2 statistic provides an estimate of the relationship between a model and a response variable. A synergistic analysis was performed to associate the trends of backscatter and multispectral bands with each other. This was conducted by determining the correlation between Sentinel-1 and Sentinel-2 products. A correlation value of one (1) indicates that a perfect positive relationship exists between the trends, a zero (0) suggests that no relationship transpires, and negative one (-1) indicates that there is a perfect inverse relationship between the trends. Table 3. shows the statistics of trees used for backtracking trends.

Table 3. Statistics of dead trees used for trends analysis

	No. of Trees	Population Proportion (%)
SAR Backscatter	24	10.5
Multispectral Bands	42	18.4
Vegetation Indices	42	18.4
Synergistic Analysis	68	29.8

2.5 Mapping of areas at-risk to stress

For a more intensive analysis of the VIs, anomaly maps were generated and were used as bases to map areas at-risk to vegetation stress. Anomaly maps present the deviation of a single satellite image from the normal or average condition and can be calculated by subtracting an average value of images from a single-date image. The anomaly formula used is shown in Equation (1), where X_n represents a single-date Sentinel-2 imagery while the latter part of the equation calculates the overall average of all the Sentinel-2 images used in this study.

$$\text{Anomaly} = X_n - \left(\frac{1}{10} \times \sum_{i=2017_1}^{2020_i} X_i\right) \quad (1)$$

To compute the relative reliability, the individual pixel values were set to one (1) if they contain numerical data and zero (0) if they represent masked areas. Using cell statistics, the sum of all 72 raster layers from nine Sentinel-2 images and eight VIs were obtained.

3.0 Results and discussion

3.1 Trends analysis

Generally, the trends for Sentinel products used in this study are expected to exhibit a continuous decline or incline while tree health deteriorates. However, slight sudden spikes can be observed on the trends within the identified timeline of interest per tree. For the backscatter analysis, these spikes are attributed to variations in surface moisture over the study area (Harfenmeister et al., 2020). Figure 2. shows sample plots of σ^0_{VH} and σ^0_{VV} backscatter.

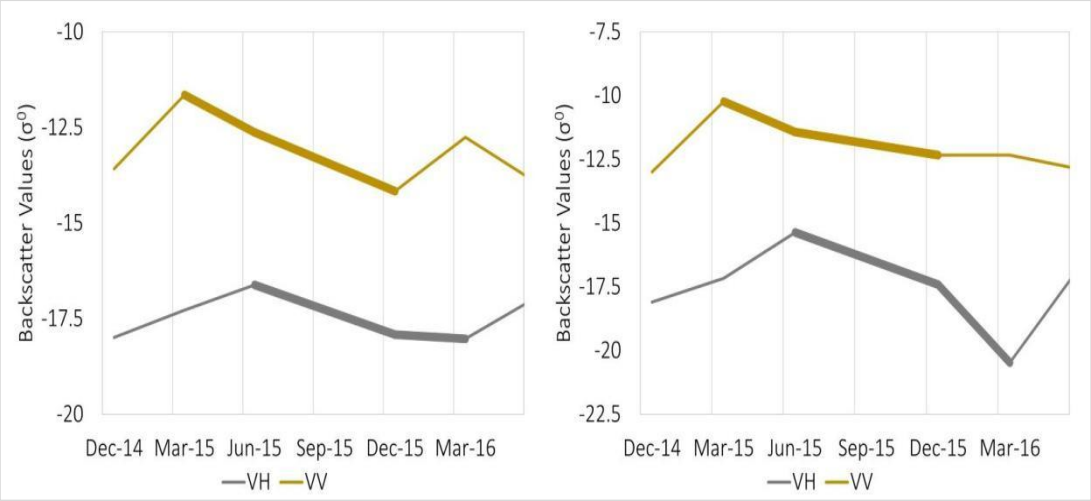

Figure 2. Sample plots displaying an earlier decline in σ^0_{VV} before σ^0_{VH} backscatter; and decline in σ^0_{VH} after σ^0_{VV} backscatter ceases to decline. The decline associated with deterioration of tree health is emphasised in thicker lines for easier visualisation.

In most cases of foliage loss, σ^0_{VH} and σ^0_{VV} exhibit simultaneous decline. However, in a likewise significant number of cases, σ^0_{VV} shows an earlier decline compared to σ^0_{VH}, and σ^0_{VH} continues to decline even after σ^0_{VV} ceases declining. For such cases, σ^0_{VH} and σ^0_{VV} decline generally take the same amount of time. Statistics of these observations are listed in Table 4.

Table 4. Statistics of observations for Sentinel-1 backtracking

Sample Size (out of 228)	Count
σ^0_{VH} and σ^0_{VV} begins declining simultaneously	32
σ^0_{VH} begins declining before σ^0_{VV}	9
σ^0_{VV} begins declining before σ^0_{VH}	27
σ^0_{VH} and σ^0_{VV} ceases declination simultaneously	27
σ^0_{VH} stops declining before σ^0_{VV} does	11
σ^0_{VV} stops declining after σ^0_{VH} does	30

Backscatter values of deteriorating pine trees in the study area show a stronger decline in the σ^0_{VV} polarisation. The differences in backscatter response intensity are attributed to limitations on σ^0_{VH} sensitivity at high altitudes. The structure of pine tree leaves also contributes to a mild σ^0_{VH} response as the presence of biomass with narrow leaves increases the absorption effect of the signal which causes a flat trend in σ^0_{VH} values (Stendardi et al.,

2019). The bands exhibiting the earliest decline are bands 5, 6, 7, 8, and 8A. Bands 2, 3, and 4, along with SWIR 1 and SWIR 2, make up the next set showing decline. Figure 3. and Figure 4. show the slope values of the overall decline and their corresponding R^2 statistic, respectively.

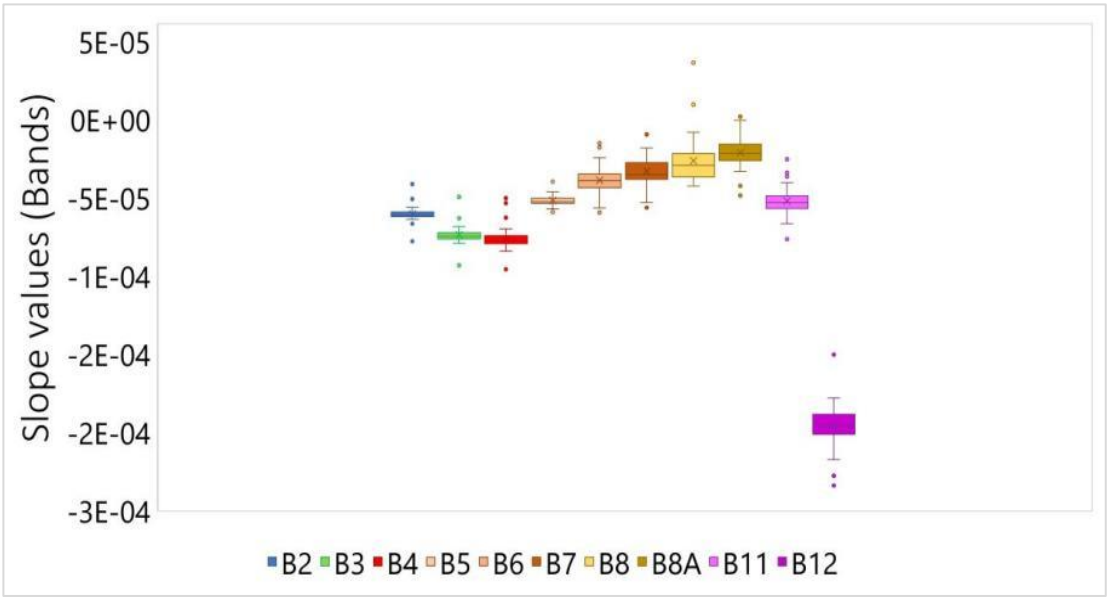

Figure 3. Box and whisker plot of the decline in band trends (slope).

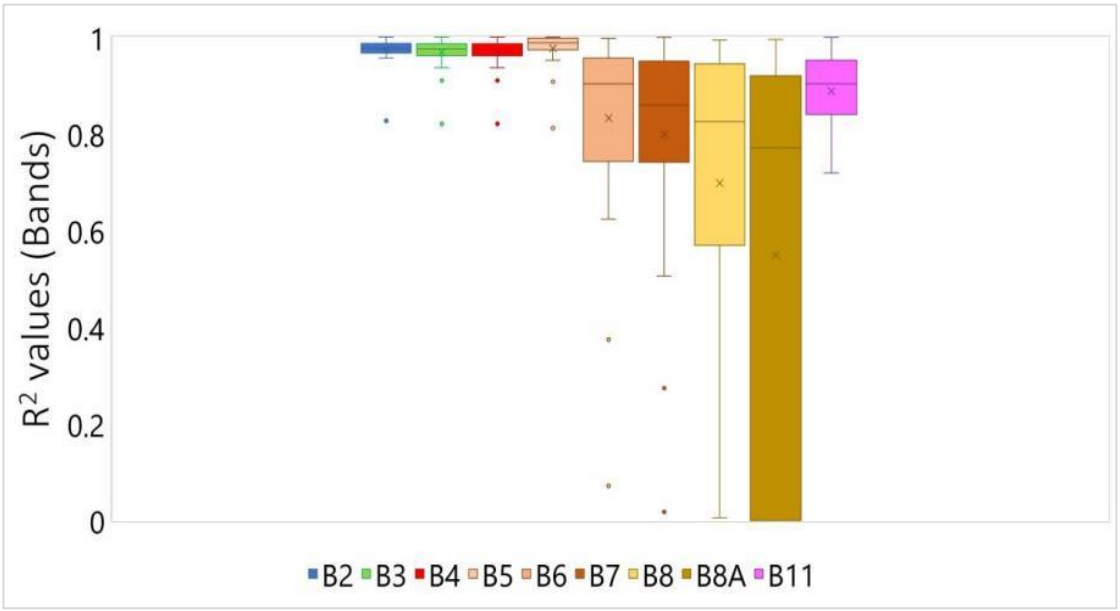

Figure 4. Box and whisker plot of the decline in band trends (R^2).

From the standard deviations in both the slope and R^2 analyses, it may be observed that bands 2, 3, 4, and 5 exhibited the most consistent amount of decline. The R^2 statistics of the said bands are also the highest among the bands. These findings indicate that the properties of

deteriorating pine trees characterised by bands 2, 3, 4, and 5 are the least influenced by environmental factors, hence, are the most robust among the bands. Meanwhile, Kumbula et al. (2019) found similar results where the most influential bands for predicting stress caused by wood boring insects are bands 5, 4, 3, 12, and 2, ranked accordingly. It was discussed in their study that there is a high correlation between red edge bands and the chlorophyll content of the leaves; hence, the spectral signature of bark beetles after chlorosis due to infestation is easily detected on the red edge spectrum. It was further explained in their study that the progression of damages in tree trunks and branches due to infestation results in foliage discoloration. As a result, there is a reduction in the absorption rates of the visible light as there are fewer green pigments available.

VIs which declines the earliest are S2REP, NDWI, and EVI. These indices are trailed by decline in MSI and GNDVI, and an increase in NDII. NDVI and IRECI, respectively, are the last to manifest decline. From inspection of their behaviours, VIs that show the smoothest decline in trends are MSI, GNDVI, and NDVI. NDII, which is expected to increase while other VIs decrease, has a smooth trend as well. Figure 5. summarised the values of slope per VI. The set of S2REP slope values has an exceedingly wide range of values which is not encompassed in the box and whisker plot; hence, it is excluded as a candidate to be a robust VI for early stress detection in pine trees. The ranges and standard deviations of their slope values indicate that the amount of decline of GNDVI is the most invariant. This is followed by NDII, EVI, and MSI, respectively. Afterwards, NDWI and NDVI equally. The VIs with small standard deviations are more sensitive to changes in stress in pine trees than other external factors over time.

R^2 values of VI decline were also arranged in a box and whisker plot (Figure 6) to estimate the relationship between VI values and their decline over time while the trees deteriorate. Since R^2 can only be computed with a minimum of three (3) pairs of x and y data points, analysis of R^2 values is only applicable to decline in S2REP, NDII, MSI, and GNDVI. R^2 values and standard deviations of VI trends indicate that NDII, MSI show better reliability than S2REP when it comes to determining presence of stress in trees.

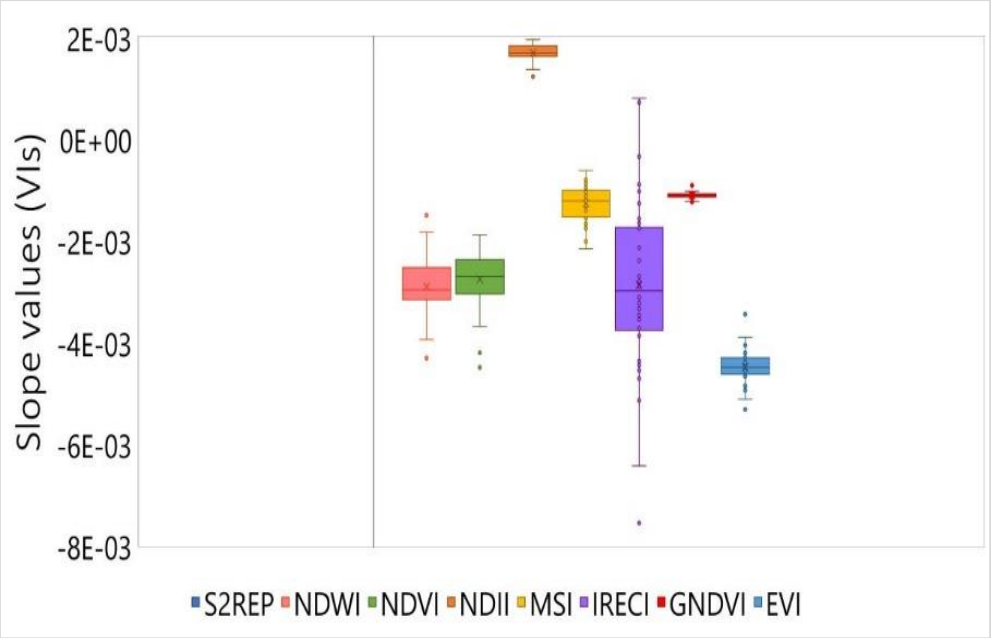

Figure 5. Box and whisker plot of VI trends (slope). The plot suggests that the VIs most sensitive to detect changes due to stress in pine trees and least affected by other external factors are ranked accordingly: GNDVI, NDII, EVI, MSI, followed equally by NDWI and NDVI.

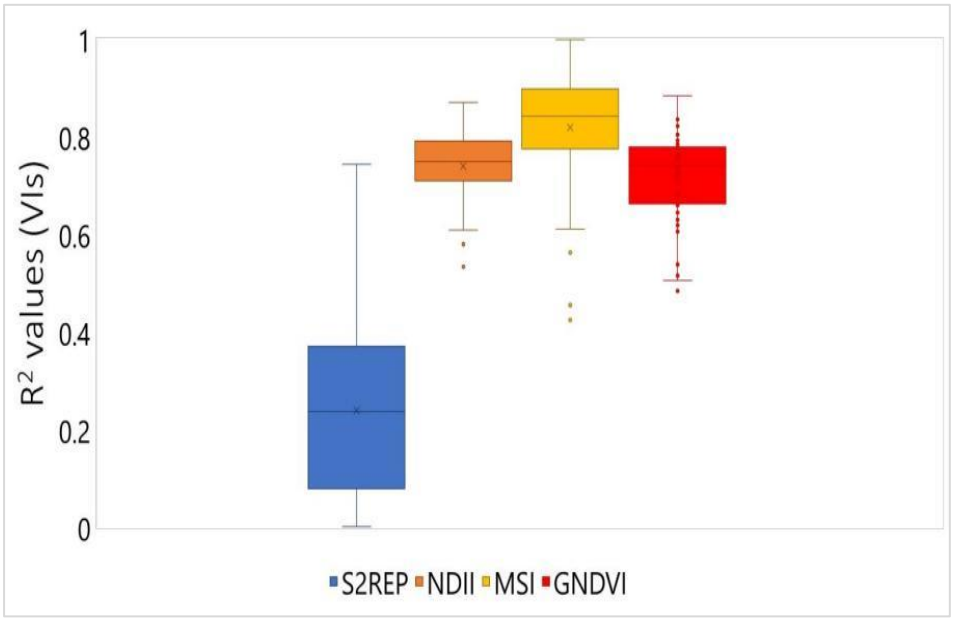

Figure 6. Box and whisker plot of the decline in VI trends (R^2). The plot suggests that NDII, MSI, and GNDVI have good reliability in determining presence of stress in pine trees.

Based on the behaviours of VI trends, their slope and R^2 values altogether, the most robust VIs to detect stress in trees are GNDVI, MSI, NDII and NDVI. Among these, GNDVI, MSI, and NDII simultaneously reflect changes in trends due to stress earlier than NDVI. Kumbula et al. (2019) confirm that GNDVI performs outstandingly in the occurrence of stress due to infestation by wood boring insects since identifying the healthy and stressed vegetation is mostly observed in the green peak and vegetation red edge region. Hawrylo et al. (2018) showed similar findings where GNDVI was identified to be more suitable than NDVI for health deterioration and defoliation assessment. The delay in NDVI decline, as the study suggests, occurs since the correlation between NDVI and health deterioration of trees are more prominent in more severe defoliation stages. Sanguesa-Barreda et al. (2014) support the finding that MSI, which is positively associated with defoliation, as well as NDII which is negatively associated with it, are robust for tracking health deterioration of trees. Specifically, for conifer forests, MSI is expected to perform better than NDVI for distinguishing damages in trees since MSI is strongly associated with decreases in canopy greenness. Recalling band trends at the onset of stress in pine stress, NIR reflectance did not show a significant response. The changes in response due to the onset of stress manifests more significantly in the green reflectance; hence, it holds up that MSI, GNDVI, and the green band are among the robust indicators of early stages of stress in pine trees.

The synergistic analysis involved examining the correlation between backscatter trends and those of multispectral bands. There was no notable correlation found between both the σ^0_{VH} and σ^0_{VV} polarisations and any of the bands (Figure 7.). Although they exhibit a positive correlation in most cases, the correlation values cluster near zero (0); hence, they are not sufficient to deem that there is a significant relationship.

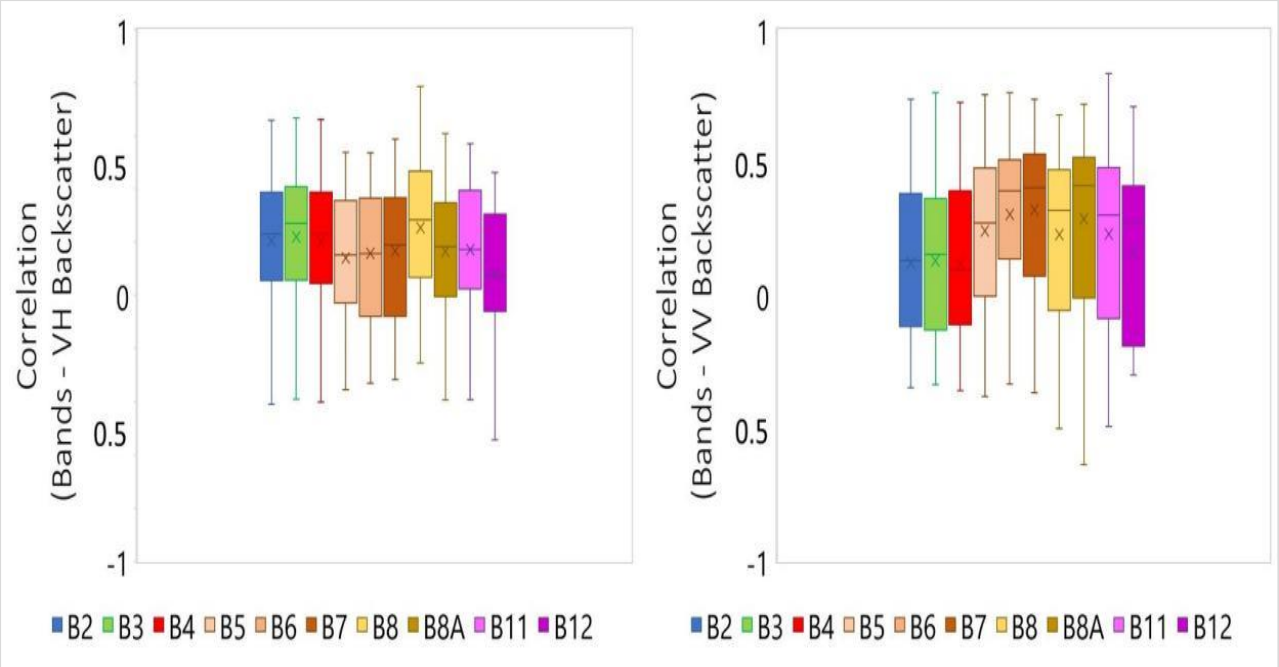

Figure 7. Correlation between bands and backscatter. All correlation values cluster near zero (0). This suggests that there is no notable correlation between both σ^0_{VH} and σ^0_{VV} backscatter and any of the bands.

VIs shows a relatively better correlation with backscatter trends than the individual bands. However, their correlation values are still insufficient to be considered as having a good relationship. This inference, however, is inapplicable to σ^0_{VV} -NDVI correlation. From Figure 8., it may be observed that among all the other pairs, σ^0_{VV} -NDVI has the best set of correlation values to a relatively considerable extent. σ^0_{VV} -NDVI has the highest positive correlation values with the smallest standard deviation. Unlike σ^0_{VV} -NDVI, a sturdy correlation does not apply to σ^0_{VH} -NDVI.

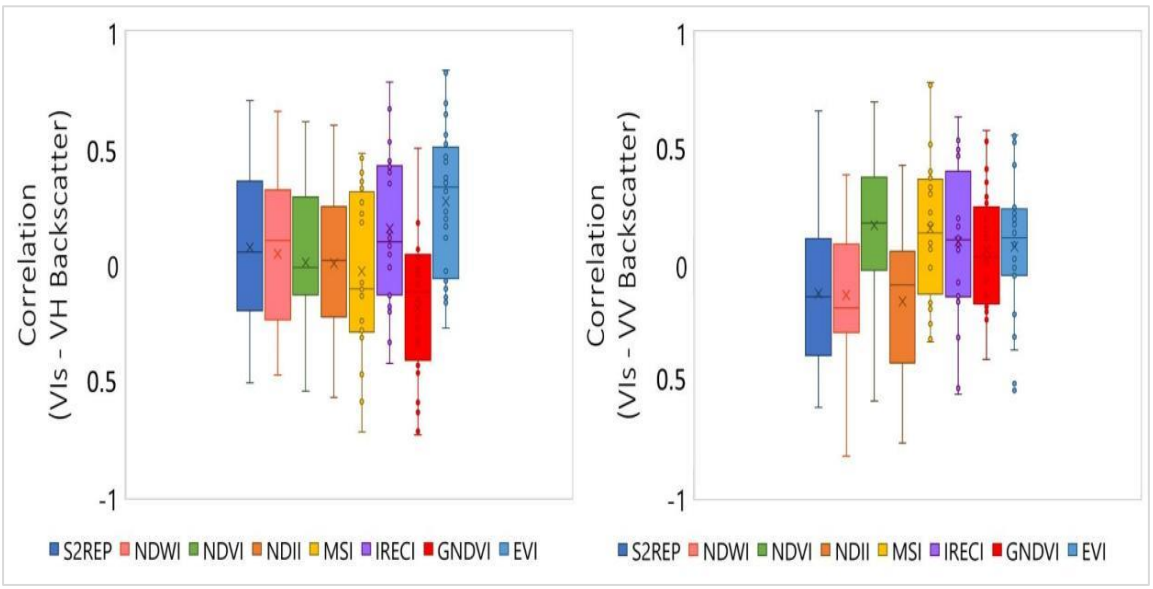

Figure 8. Correlation between vegetation indices and backscatter. σ^0_{VV} -NDVI exhibits a significant positive correlation with each other. The pairs of σ^0_{VH} -IRECI, σ^0_{VH} -EVI, σ^0_{VV} -MSI, and σ^0_{VV} -IRECI also cluster at high positives but are not as robust as suggested by their standard deviations.

These findings may be attributed to the possibility that the contribution of bare soil and a vegetation structure of short and thin leaves increases the sensitivity to variations in the water content of soil, instead of vegetation cover, as discussed by Stendardi et al. (2019). The correlation values of σ^0_{VH} -IRECI, σ^0_{VH} -EVI, σ^0_{VV} -MSI, and σ^0_{VV} -IRECI cluster at high positives; however, their high standard deviations and numerous outliers reduce their robustness.

3.2 Map of areas at-risk to stress

The sum of all negative anomalies exclusively produces a map which represents areas with pixels containing the most negative anomalies (Figure 9.). All values in the resulting map indicate stress or deterioration of vegetation health. Moreover, the areas identified to be at risk are overlaid with the location of dead trees. Table 5. shows the statistics of dead trees within the study area. From the sum of the 72 raster layers, the maximum number of pixels obtained is 47; hence, the maximum relative reliability percentage is computed at 65.3%.

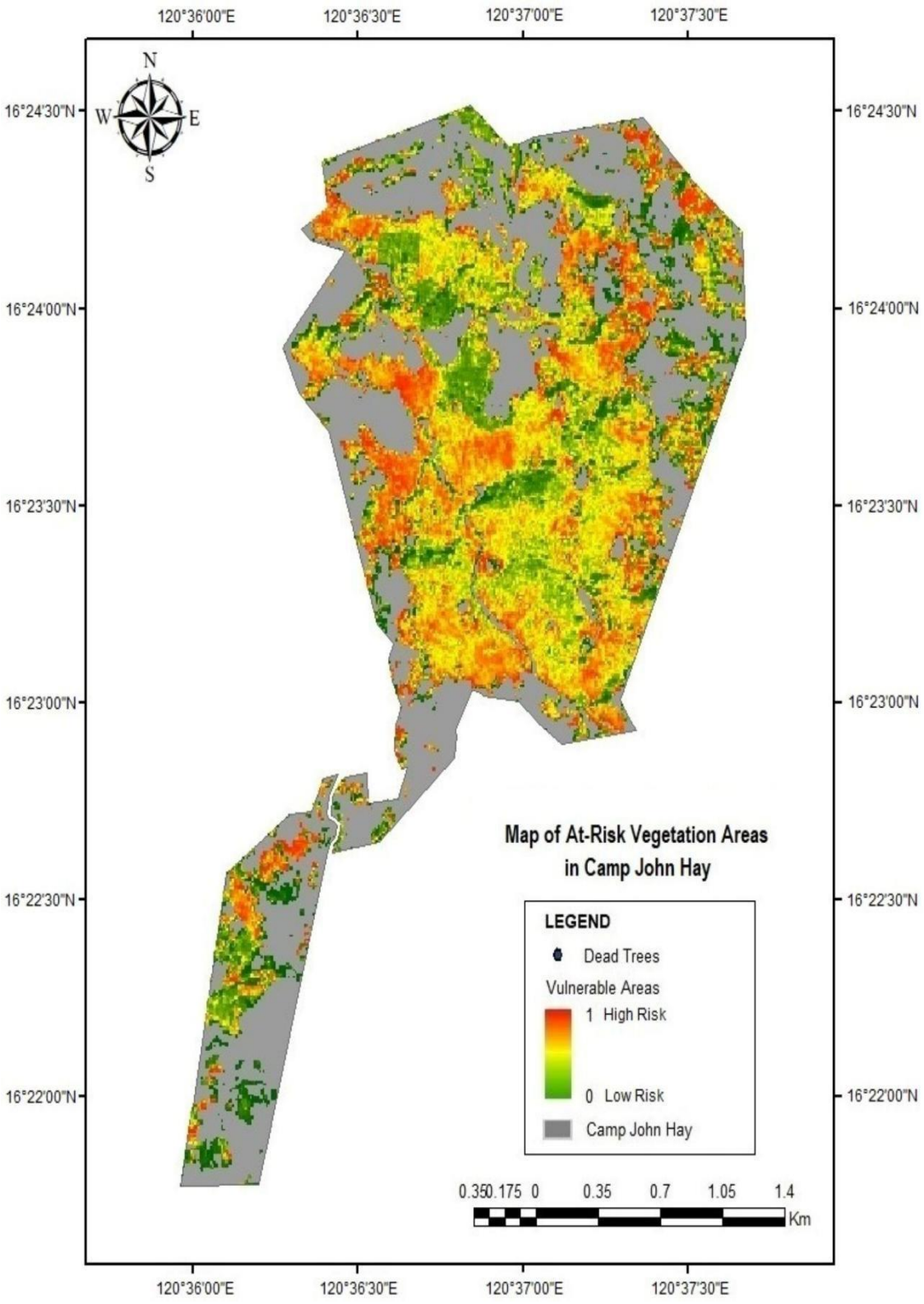

Figure 9. Map of at-risk vegetation areas.

Table 5. Statistics of dead trees plotted with at-risk areas.

	No. of Dead Trees	Percentage (out of 228 trees)
High risk areas	24	10.5
Low risk areas	42	18.4
No Data	68	29.8

In summary, the potential of Sentinel-1 and Sentinel-2 satellite systems proved adequate to assess pine forest condition via trends analysis of products derived from Sentinel-1 and Sentinel-2 imagery. Based on the trend behaviours of backscatter signals, bands, and VIs, it was found that the onset of stress in pine trees manifests more significantly in the green reflectance than in NIR. From the synergistic analysis of Sentinel-1 and Sentinel-2 products, it was found that the most robust product for the early detection of stress in pine trees is band 5 (red edge), followed by GNDVI, NDII, MSI, and bands 2, 3, and 4 of equal importance. NDVI decline occurs in the more advanced stages of tree health deterioration. NDVI was found to be well-correlated with σ^0_{VV} backscatter; hence, they exhibit concurrent decline. And σ^0_{VH} backscatter is the last to manifest a decline in trends. These delays in trend decline are clearly manifested in intervals of three (3) months. Negative and positive anomalies were separated and processed individually to generate the map of at-risk vegetation areas. The sum of all negative anomalies in the images were used to locate areas susceptible to vegetation stress, while the sum of all positive anomalies located the areas with relatively stable conditions throughout the period covered in this study. This study shows that the integration of Sentinel-1 SAR and Sentinel-2 multispectral imagery is a promising approach in the comprehensive assessment of pine forest condition towards the monitoring and early stress detection.

Acknowledgements

This study was funded and supported by the Department of Science and Technology Science Education Institute. We thank the Watershed and Water Resources Research, Development and Extension Center (WWRRDEC) in Baguio City, as well as John Hay Management Corporation (JHMC) for their hospitality and generosity in sharing data essential for the execution of this study. We also extend our gratitude to Geospatial Assessment and Modelling of Urban Heat Islands in Philippine Cities (Project GUHeat) of UP Training Center for Applied Geodesy and

Photogrammetry (UP TCAGP) and Department of Science and Technology – Philippine Council for Industry, Energy and Emerging Technology Research and Development (DOST-PCIEERD) for accommodating our consultations and providing supplementary lectures which helped in the improvement of this study.

References

Abdullah, H., Darvishzadeh, R., Skidmore, A.K., Groen, T.A. and Heurich, M., 2018. *"European Spruce Bark Beetle (Ips Typographus, L.) Green Attack Affects Foliar Reflectance and Biochemical Properties".* International Journal of Applied Earth Observation and Geoinformation, 64, :199-209.

Arellano, C.M., Maralit, A.A., Paringit, E.C., Sarmiento, C.J., Faelga, R.A., Tandoc, F.A., Vidad, C., Lopez, R. and Pamittan, F.J., 2019. *"Multi-Temporal Analysis of Dense and Sparse Forests'radar Backscatter Using Sentinel-1a Collection in Google Earth Engine".* International Archives of the Photogrammetry, Remote Sensing & Spatial Information Sciences.

Bao, N., Li, W., Gu, X. and Liu, Y., 2019. *"Biomass Estimation for Semiarid Vegetation and Mine Rehabilitation Using Worldview-3 and Sentinel-1 SAR Imagery".* Remote Sensing, 11(23): 2855.

Braun, A., Fakhri, F. and Hochschild, V., 2019. *"Refugee Camp Monitoring and Environmental Change Assessment of Kutupalong, Bangladesh, Based on Radar Imagery of Sentinel-1 and ALOS-2"*. Remote Sensing, 11(17): 2047.

Dostálová, A., Hollaus, M., Milenković, M. and Wagner, W., 2016. *"Forest Area Derivation from Sentinel-1 Data"*. ISPRS Annals of the Photogrammetry, Remote Sensing and Spatial Information Sciences, 3, :227.

Frampton, W.J., Dash, J., Watmough, G. and Milton, E.J., 2013. *"Evaluating the Capabilities of Sentinel-2 for Quantitative Estimation of Biophysical Variables in Vegetation".* ISPRS Journal of Photogrammetry and Remote Sensing, 82, :83-92.

Harfenmeister, K., Spengler, D. and Weltzien, C., 2019. *"Analyzing Temporal and Spatial Characteristics of Crop Parameters Using Sentinel-1 Backscatter Data".* Remote Sensing, 11(13): 1569.

Hawryło, P., Bednarz, B., Wężyk, P. and Szostak, M., 2018. *"Estimating Defoliation of Scots Pine Stands Using Machine Learning Methods and Vegetation Indices of Sentinel-2".* European Journal of Remote Sensing, 51(1): 194-204.

Kumbula, S.T., Mafongoya, P., Peerbhay, K.Y., Lottering, R.T. and Ismail, R., 2019. *"Using Sentinel-2 Multispectral Images to Map the Occurrence of The Cossid Moth (Coryphodema Tristis) in Eucalyptus Nitens Plantations of Mpumalanga, South Africa"*. Remote Sensing, 11(3): 278.

Lausch, A., Erasmi, S., King, D.J., Magdon, P. and Heurich, M., 2016. *"Understanding Forest Health with Remote Sensing-Part I—A Review of Spectral Traits, Processes and Remote-Sensing Characteristics"*. Remote Sensing, 8(12): 1029.

Lausch, A., Erasmi, S., King, D.J., Magdon, P. and Heurich, M., 2017. *"Understanding Forest Health with Remote Sensing-Part II—A Review of Approaches and Data Models".* Remote Sensing, 9(2): 129.

Parao, M.R., Untalan, P.P., Ligat, B.S., Pagadan, C.S. and Tanguid, L.B., 2019. *"Damage Assessment of Bark Beetle Infestations on Benguet Pine (Pinus kesiya Royle ex Gordon) in Camp John Hay, Baguio City, Philippines".* Mountain Journal of Science and Interdisciplinary Research (formerly Benguet State University Research Journal), 79(2): 35-49.

Sangüesa-Barreda, G., Camarero, J.J., García-Martín, A., Hernández, R. and de la Riva, J., 2014. *"Remote-Sensing and Tree-Ring Based Characterization of Forest Defoliation and Growth Loss Due to The Mediterranean Pine Processionary Moth".* Forest Ecology and Management, 320, :171-181.

Semeraro, T., Luvisi, A., Lillo, A.O., Aretano, R., Buccolieri, R. and Marwan, N., 2020. *"Recurrence Analysis of Vegetation Indices for Highlighting the Ecosystem Response to Drought Events: An Application to the Amazon Forest"*. Remote Sensing, 12(6): 907.

Stendardi, L., Karlsen, S.R., Niedrist, G., Gerdol, R., Zebisch, M., Rossi, M. and Notarnicola, C., 2019. *"Exploiting Time Series of Sentinel-1 and Sentinel-2 Imagery to Detect Meadow Phenology in Mountain Regions"*. Remote Sensing, 11(5): 542.

Zhang, T., Su, J., Liu, C., Chen, W.H., Liu, H. and Liu, G., 2017, September. *"Band Selection in Sentinel-2 Satellite for Agriculture Applications"*. In 2017 23rd International Conference on Automation and Computing (ICAC): 1-6. IEEE.